CRAMÉR-RAO BOUND FOR DOA ESTIMATORS UNDER THE PARTIAL RELAXATION FRAMEWORK

Minh Trinh-Hoang[⋆] *Mats Viberg*[‡] *Marius Pesavento*[⋆]

[⋆] Communication Systems Group, Darmstadt University of Technology, Darmstadt, Germany
[‡] Blekinge Institute of Technology, Karlskrona, Sweden

ABSTRACT

In this paper, the Cramér-Rao Bound for the Direction-of-Arrival parameter under the partial relaxation framework is derived. We introduce a non-redundant parameterization of the signal model corresponding to the partial relaxation framework, in which the array structure in part of the steering matrix is neglected while the rank of the relaxed steering matrix is maintained. We prove that the stochastic Cramér-Rao Bound for the Direction-of-Arrival parameter under the partial relaxation signal model is lower-bounded by that of the conventional stochastic Cramér-Rao Bound. Furthermore, we prove that the partial relaxation estimator for the Weighted Subspace Fitting criterion asymptotically achieves the conventional Cramér-Rao Bound in the case of uncorrelated source signals.

***Index Terms*—** DOA Estimation, Cramér-Rao Bound, Partial Relaxation, Non-redundant Parameterization, Mean-squared Error.

1. INTRODUCTION

Partial relaxation (PR) has been recently introduced as a new framework for the task of Direction-of-Arrival (DOA) estimation. The idea of partial relaxation is to treat the steering matrix as an element of a relaxed steering manifold where the sensor array structure of only one direction is maintained. Methods developed under the PR framework exhibit improved performance with respect to the conventional spectral-search algorithm at comparable computational complexity. Particularly, the PR method based on the covariance fitting criterion possess exceptional threshold performance which is comparable to that of the Maximum Likelihood estimator [1, 2, 3].

Comparing to DOA estimators utilizing the full dimensional search, e.g., Maximum Likelihood estimators [4, 5], due to the relaxation of the steering structure and thus implying a model mismatch with the true model, degraded performance of PR methods in terms of DOAs estimation error is predicted. On the other hand, since the interfering effects of neighboring source signals are partially considered in the PR framework, an improvement in the estimation error is expected in the case of PR methods when comparing with estimators utilizing the single-source approximation in the least-square formulation[3, Sec. III], e.g., MUSIC[6]. In the literature, this conjecture has only been numerically confirmed in certain scenarios in [3], and the theoretical difference in the asymptotic estimation error between PR estimators and conventional counterparts has not been analyzed. Furthermore, the Cramér-Rao Bound (CRB) for the DOA parameter under the PR framework, which represents the lower bound on the asymptotic estimation error of all unbiased PR estimators, has neither been derived nor compared with the conventional stochastic CRB [7, 8, 9].

In this paper, the asymptotic behavior of the DOA estimators under the PR framework is investigated through the CRB analysis [10, 11, 12]. First, the conventional signal model for the task of DOA estimation is introduced in Section 2. A brief introduction of the PR model and the corresponding parameterization of the covariance matrix of the received signal for the PR signal model are presented in Section 3. In Section 4, a closed-form formula of the CRB for the DOA parameter under the PR signal model is derived. Theoretical implications and numerical results regarding the performance of estimators using the conventional and the PR signal model are presented in Sections 5 and 6, respectively. In Section 7, some concluding remarks are made and extensions to future research are discussed.

2. CONVENTIONAL SIGNAL MODEL

Consider an array of M sensors receiving N narrowband signals emitted from sources with corresponding unknown DOAs $\boldsymbol{\theta} = [\theta_1, \ldots, \theta_N]^{\mathrm{T}}$. We assume that the number of sources N is known, and $N < M$. The sensor measurement vector $\boldsymbol{x}(t) = [x_1(t), \ldots, x_M(t)]^{\mathrm{T}} \in \mathbb{C}^{M\times 1}$ in the baseband at time instant t is modeled as

$$\boldsymbol{x}(t) = \boldsymbol{A}(\boldsymbol{\theta})\boldsymbol{s}(t) + \boldsymbol{n}(t) \text{ for } t = 1, \ldots, T, \tag{1}$$

where $\boldsymbol{s}(t) = [s_1(t), \ldots, s_N(t)]^{\mathrm{T}} \in \mathbb{C}^{N\times 1}$ denotes the baseband source signal vector from N sources. We assume that the transmit signal vector $\boldsymbol{s}(t)$ is Gaussian distributed, i.e., $\boldsymbol{s}(t) \sim \mathcal{N}_C(\boldsymbol{0}, \boldsymbol{P})$ with rank $(\boldsymbol{P}) = N$. Further, $\boldsymbol{n}(t) \in \mathbb{C}^{M\times 1}$ represents the additive circularly complex Gaussian noise vector at the sensor array with the noise covariance matrix $\nu \boldsymbol{I}_M$. The steering matrix $\boldsymbol{A}(\boldsymbol{\theta}) \in \mathbb{C}^{M\times N}$ in (1), which is assumed to have full column rank, is given by

$$\boldsymbol{A}(\boldsymbol{\theta}) = [\boldsymbol{a}(\theta_1), \ldots, \boldsymbol{a}(\theta_N)], \tag{2}$$

where $\boldsymbol{a}(\theta_n)$ denotes the sensor array response for the DOA θ_n. Assuming that the source signals and the noise are uncorrelated, the received signal $\boldsymbol{x}(t)$ is also Gaussian distributed with zero mean and covariance matrix $\boldsymbol{R}$, where the covariance matrix $\boldsymbol{R} \in \mathbb{C}^{M\times M}$ is given by

$$\boldsymbol{R} = \mathbb{E}\left\{\boldsymbol{x}(t)\boldsymbol{x}(t)^{\mathrm{H}}\right\} = \boldsymbol{A}\boldsymbol{P}\boldsymbol{A}^{\mathrm{H}} + \nu \boldsymbol{I}_M. \tag{3}$$

3. PARAMETERIZATION OF THE PARTIAL RELAXATION MODEL

As mentioned in [1, 3], the signal model for the PR model is similar to the conventional counterpart in (1). However, the structure of the steering matrix is partially relaxed, i.e., $\boldsymbol{A} \in \bar{\mathcal{A}}_N$ where the relaxed array manifold $\bar{\mathcal{A}}_N$ is defined as:

$$\bar{\mathcal{A}}_N = \left\{ \boldsymbol{A} = [\boldsymbol{a}(\theta), \boldsymbol{B}] \middle| \text{rank}(\boldsymbol{A}) = N, \boldsymbol{B} \in \mathbb{C}^{M\times(N-1)} \right\}, \tag{4}$$

and $\theta \in \{\theta_1, \dots, \theta_N\}$ is the desired direction whose parameterization is maintained. Since the received signal is Gaussian distributed with zero mean, all information is concentrated in the covariance matrix $\boldsymbol{R}$. As a consequence, in order to derive the CRB from the received signal under the PR model, we introduce a compact non-redundant parameterization of the received covariance matrix $\boldsymbol{R}$ in (3) under the assumption $\boldsymbol{A} \in \bar{\mathcal{A}}_N$ as described in the following. We note that the rank condition in (4) implies that there exists an invertible minor square matrix of $\boldsymbol{A}$ with dimension $N \times N$. By re-indexing the sensors if necessary, we assume that, for the following matrix partition

$$\boldsymbol{A} = \begin{bmatrix} a_1(\theta) & \boldsymbol{b}_1^{\mathrm{T}} \\ \boldsymbol{a}_2(\theta) & \boldsymbol{B}_2 \\ \boldsymbol{a}_3(\theta) & \boldsymbol{B}_3 \end{bmatrix} \begin{matrix} \}\, 1 \\ \}\, (M-N) \\ \}\, (N-1) \end{matrix} \tag{5}$$

the minor block matrix $\begin{bmatrix} a_1(\theta) & \boldsymbol{b}_1^{\mathrm{T}} \\ \boldsymbol{a}_3(\theta) & \boldsymbol{B}_3 \end{bmatrix}$ is invertible with $a_1(\theta) \neq 0$, and therefore the inverse $\left(\boldsymbol{B}_3 - \boldsymbol{a}_3 a_1^{-1} \boldsymbol{b}_1^{\mathrm{T}}\right)^{-1}$ exists. By introducing the invertible transformation matrix $\boldsymbol{T}$:

$$\boldsymbol{T} = \begin{bmatrix} 1 & -a_1^{-1}\boldsymbol{b}_1^{\mathrm{T}} \left(\boldsymbol{B}_3 - \boldsymbol{a}_3 a_1^{-1} \boldsymbol{b}_1^{\mathrm{T}}\right)^{-1} \\ \boldsymbol{0} & \left(\boldsymbol{B}_3 - \boldsymbol{a}_3 a_1^{-1} \boldsymbol{b}_1^{\mathrm{T}}\right)^{-1} \end{bmatrix}, \tag{6}$$

with the shorthand notation $\boldsymbol{a} = \boldsymbol{a}(\theta) = \left[a_1, \boldsymbol{a}_2^{\mathrm{T}}, \boldsymbol{a}_3^{\mathrm{T}}\right]^{\mathrm{T}}$, the signal model in (1) is rewritten as

$$\boldsymbol{x}(t) = \bar{\boldsymbol{A}}\bar{\boldsymbol{s}}(t) + \boldsymbol{n}(t), \tag{7}$$

where the transformed steering matrix $\bar{\boldsymbol{A}}$ and the transformed transmit signal $\bar{\boldsymbol{s}}(t)$ are defined as:

$$\bar{\boldsymbol{A}} = \boldsymbol{A}\boldsymbol{T} = \begin{bmatrix} a_1 & \boldsymbol{0}^{\mathrm{T}} \\ \boldsymbol{a}_2 & \bar{\boldsymbol{B}} \\ \boldsymbol{a}_3 & \boldsymbol{I}_{N-1} \end{bmatrix} \quad \text{and} \quad \bar{\boldsymbol{s}}(t) = \boldsymbol{T}^{-1}\boldsymbol{s}(t). \tag{8}$$

The reduced interference matrix $\bar{\boldsymbol{B}} \in \mathbb{C}^{(M-N)\times(N-1)}$ in (8) is computed as

$$\bar{\boldsymbol{B}} = \left(\boldsymbol{B}_2 - \boldsymbol{a}_2 a_1^{-1} \boldsymbol{b}_1^{\mathrm{T}}\right)\left(\boldsymbol{B}_3 - \boldsymbol{a}_3 a_1^{-1} \boldsymbol{b}_1^{\mathrm{T}}\right)^{-1}. \tag{9}$$

As a result, any relaxed steering matrix $\boldsymbol{A} \in \bar{\mathcal{A}}_N$ in (4) can be uniquely parameterized by the desired DOA θ, the unstructured matrix $\bar{\boldsymbol{B}}$ and the transformation matrix $\boldsymbol{T}$. Applying the transformation in (8) to (3) and noting that the transformed transmit signal $\bar{\boldsymbol{s}}(t)$ is Gaussian distributed with zero mean, we obtain

$$\boldsymbol{R} = \bar{\boldsymbol{A}}\bar{\boldsymbol{P}}\bar{\boldsymbol{A}}^{\mathrm{H}} + \nu \boldsymbol{I}_M, \tag{10}$$

where $\bar{\boldsymbol{A}}$ is defined in (8) and $\bar{\boldsymbol{P}} = \boldsymbol{T}^{-1}\boldsymbol{P}\boldsymbol{T}^{-\mathrm{H}}$ is the transformed transmit covariance matrix. Clearly, the parameterization of $\boldsymbol{R}$ does not require the knowledge of either $\boldsymbol{T}$ or $\boldsymbol{P}$ but only the Hermitian matrix $\bar{\boldsymbol{P}}$. Motivated by this observation, we collect all parameters required to describe the covariance matrix $\boldsymbol{R}$ in the PR model defined in (10) as follows

$$\boldsymbol{\alpha} = \left[\theta, \boldsymbol{\epsilon}^{\mathrm{T}}, \boldsymbol{\eta}^{\mathrm{T}}, \bar{\boldsymbol{p}}^{\mathrm{T}}, \nu\right]^{\mathrm{T}}, \tag{11}$$

where $\boldsymbol{\alpha}$ is the parameter vector, $\epsilon_{(k,l)} = \text{Re}\left\{\bar{B}_{kl}\right\}$ and

$$\boldsymbol{\epsilon} = \left[\epsilon_{(1,1)}, \dots, \epsilon_{(M-N,1)}, \dots\dots, \epsilon_{(M-N,N-1)}\right]^{\mathrm{T}} \tag{12}$$

contains the real part of the reduced interference parameters in $\bar{\boldsymbol{B}}$. In the same manner, we define $\eta_{(k,l)} = \text{Im}\left\{\bar{B}_{kl}\right\}$ and

$$\boldsymbol{\eta} = \left[\eta_{(1,1)}, \dots, \eta_{(M-N,1)}, \dots\dots, \eta_{(M-N,N-1)}\right]^{\mathrm{T}} \tag{13}$$

contains the imaginary part of the interference parameters. $\bar{\boldsymbol{p}} \in \mathbb{R}^{N^2\times 1}$ is obtained from $\left\{\bar{P}_{nn}\right\}, \text{Re}\left\{\bar{P}_{mn}\right\}$ and $\text{Im}\left\{\bar{P}_{mn}\right\}$ for $1 \le m, n \le N$ and $m < n$. It is not difficult to show that the parameterization in (11) is unique, and thus the CRB exists for the corresponding parameters [13]. Using the non-redundant parameterization in (11), in the next section, the CRB corresponding to the desired parameter θ is derived.

4. DERIVATION OF THE CRAMÉR-RAO BOUND FOR THE PARAMETER θ

Inspired by the work in [8, 14], in this section, we derive the CRB for the parameter θ of the PR model case as given in (7) and (10). We assume that, the inverse matrices which appear in the following derivation exist. In accordance with the parameterization in (11), the element on the p-th row and q-th column of the inverse CRB $\boldsymbol{C}^{-1} = \boldsymbol{\Sigma}$ for the parameters $\boldsymbol{\beta} = \left[\theta \middle| \boldsymbol{\epsilon}^{\mathrm{T}} \middle| \boldsymbol{\eta}^{\mathrm{T}}\right]^{\mathrm{T}}$ is given by [8, Eqs. (15)-(17), (31)]

$$\Sigma_{pq} = \frac{2T}{\nu}\text{Re}\left\{\text{tr}\left(\bar{\boldsymbol{P}}\bar{\boldsymbol{A}}^{\mathrm{H}}\boldsymbol{R}^{-1}\bar{\boldsymbol{A}}\bar{\boldsymbol{P}}\frac{d\bar{\boldsymbol{A}}}{d\beta_p}^{\mathrm{H}}\boldsymbol{\Pi}_{\bar{\boldsymbol{A}}}^{\perp}\frac{d\bar{\boldsymbol{A}}}{d\beta_q}\right)\right\}, \tag{14}$$

where $\boldsymbol{\Pi}_{\bar{\boldsymbol{A}}}^{\perp} = \boldsymbol{I} - \bar{\boldsymbol{A}}\left(\bar{\boldsymbol{A}}^{\mathrm{H}}\bar{\boldsymbol{A}}\right)^{-1}\bar{\boldsymbol{A}}^{\mathrm{H}}$, and the vectors $\boldsymbol{\epsilon}$ and $\boldsymbol{\eta}$ are defined in (12) and (13), respectively. The CRB matrix $\boldsymbol{C}$ is partitioned in accordance with the partition of $\boldsymbol{\beta}$ as follows

$$\boldsymbol{C}^{-1} = \begin{bmatrix} C_{\theta\theta} & \boldsymbol{C}_{\theta\boldsymbol{\epsilon}} & \boldsymbol{C}_{\theta\boldsymbol{\eta}} \\ \boldsymbol{C}_{\boldsymbol{\epsilon}\theta} & \boldsymbol{C}_{\boldsymbol{\epsilon}\boldsymbol{\epsilon}} & \boldsymbol{C}_{\boldsymbol{\epsilon}\boldsymbol{\eta}} \\ \boldsymbol{C}_{\boldsymbol{\eta}\theta} & \boldsymbol{C}_{\boldsymbol{\eta}\boldsymbol{\epsilon}} & \boldsymbol{C}_{\boldsymbol{\eta}\boldsymbol{\eta}} \end{bmatrix}^{-1} = \begin{bmatrix} \Sigma_{\theta\theta} & \boldsymbol{\Sigma}_{\theta\boldsymbol{\epsilon}} & \boldsymbol{\Sigma}_{\theta\boldsymbol{\eta}} \\ \boldsymbol{\Sigma}_{\boldsymbol{\epsilon}\theta} & \boldsymbol{\Sigma}_{\boldsymbol{\epsilon}\boldsymbol{\epsilon}} & \boldsymbol{\Sigma}_{\boldsymbol{\epsilon}\boldsymbol{\eta}} \\ \boldsymbol{\Sigma}_{\boldsymbol{\eta}\theta} & \boldsymbol{\Sigma}_{\boldsymbol{\eta}\boldsymbol{\epsilon}} & \boldsymbol{\Sigma}_{\boldsymbol{\eta}\boldsymbol{\eta}} \end{bmatrix}. \tag{15}$$

We compute the elements of each individual matrix block independently. The entry $\Sigma_{\theta\theta}$ is computed from (14) as

$$\Sigma_{\theta\theta} = \frac{2T}{\nu}\text{Re}\left\{\boldsymbol{e}_1^{\mathrm{H}}\bar{\boldsymbol{P}}\bar{\boldsymbol{A}}^{\mathrm{H}}\boldsymbol{R}^{-1}\bar{\boldsymbol{A}}\bar{\boldsymbol{P}}\boldsymbol{e}_1\boldsymbol{d}^{\mathrm{H}}\boldsymbol{\Pi}_{\bar{\boldsymbol{A}}}^{\perp}\boldsymbol{d}\right\}, \tag{16}$$

where $\boldsymbol{d} = \dfrac{d\boldsymbol{a}(\theta)}{d\theta}$. With the definition

$$\bar{\boldsymbol{M}} = \left(\bar{\boldsymbol{P}}\bar{\boldsymbol{A}}^{\mathrm{H}}\boldsymbol{R}^{-1}\bar{\boldsymbol{A}}\bar{\boldsymbol{P}}\right)^{\mathrm{T}} = \begin{bmatrix} \bar{M}_{11} & \bar{\boldsymbol{M}}_{21}^{\mathrm{H}} \\ \bar{\boldsymbol{M}}_{21} & \bar{\boldsymbol{M}}_{22} \end{bmatrix}, \tag{17}$$

the element $\Sigma_{\theta\theta}$ is compactly written as

$$\Sigma_{\theta\theta} = \frac{2T}{\nu}\text{Re}\left\{\bar{M}_{11}\boldsymbol{d}^{\mathrm{H}}\boldsymbol{\Pi}_{\bar{\boldsymbol{A}}}^{\perp}\boldsymbol{d}\right\}. \tag{18}$$

Next, we compute $\boldsymbol{\Sigma}_{\theta\boldsymbol{\epsilon}} = \left[\Sigma_{\theta\epsilon_{(1,1)}}, \dots, \Sigma_{\theta\epsilon_{(M-N,N-1)}}\right]$. Each element $\Sigma_{\theta\epsilon_{(k,l)}}$ is computed using (14) by setting $\beta_p = \theta$ and $\beta_q = \epsilon_{(k,l)} = \text{Re}\left\{\bar{B}_{kl}\right\}$ to obtain

$$\Sigma_{\theta\epsilon_{(k,l)}} = \frac{2T}{\nu}\mathrm{Re}\left\{\boldsymbol{e}_{l+1}^{\mathrm{H}}\bar{\boldsymbol{P}}^{\mathrm{H}}\bar{\boldsymbol{A}}^{\mathrm{H}}\boldsymbol{R}^{-1}\bar{\boldsymbol{A}}\bar{\boldsymbol{P}}\boldsymbol{e}_1\boldsymbol{d}^{\mathrm{H}}\boldsymbol{\Pi}_{\bar{\boldsymbol{A}}}^{\perp}\boldsymbol{e}_{k+1}\right\}, \tag{19}$$

where $\boldsymbol{e}_k$ is an elementary vector with conformable size whose k-th element is one and the remaining are zeros. The expression in (19) is rewritten in matrix form as

$$\boldsymbol{\Sigma}_{\theta\boldsymbol{\epsilon}} = \boldsymbol{\Sigma}_{\boldsymbol{\epsilon}\theta}^{\mathrm{T}} = \frac{2T}{\nu}\mathrm{Re}\left\{\bar{\boldsymbol{M}}_{21}^{\mathrm{H}} \otimes \left(\boldsymbol{d}^{\mathrm{H}}\boldsymbol{\Pi}_{\bar{\boldsymbol{A}}}^{\perp}\boldsymbol{J}\right)\right\}, \tag{20}$$

where $\boldsymbol{J} = [\boldsymbol{e}_2, \ldots, \boldsymbol{e}_{M-N}] \in \mathbb{R}^{M\times(M-N-1)}$ is the selection matrix and $\bar{\boldsymbol{M}}_{12}$ is defined as in (17) and $\otimes$ denotes the Kronecker product. Similarly, the compact formula for the block $\boldsymbol{\Sigma}_{\theta\boldsymbol{\eta}}$ is expressed as

$$\boldsymbol{\Sigma}_{\theta\boldsymbol{\eta}} = \boldsymbol{\Sigma}_{\boldsymbol{\eta}\theta}^{\mathrm{T}} = \frac{2}{\nu}\mathrm{Re}\left\{j\bar{\boldsymbol{M}}_{21}^{\mathrm{H}} \otimes \left(\boldsymbol{d}^{\mathrm{H}}\boldsymbol{\Pi}_{\bar{\boldsymbol{A}}}^{\perp}\boldsymbol{J}\right)\right\}. \tag{21}$$

Performing the same procedure for the remaining blocks, we obtain

$$\boldsymbol{\Sigma}_{\boldsymbol{\epsilon\epsilon}} = \boldsymbol{\Sigma}_{\boldsymbol{\eta\eta}} = \frac{2T}{\nu}\mathrm{Re}\left\{\bar{\boldsymbol{M}}_{22} \otimes \left(\boldsymbol{J}^{\mathrm{H}}\boldsymbol{\Pi}_{\bar{\boldsymbol{A}}}^{\perp}\boldsymbol{J}\right)\right\}, \tag{22}$$

$$\boldsymbol{\Sigma}_{\boldsymbol{\epsilon\eta}} = \boldsymbol{\Sigma}_{\boldsymbol{\eta\epsilon}}^{\mathrm{T}} = \frac{2T}{\nu}\mathrm{Re}\left\{j\bar{\boldsymbol{M}}_{22} \otimes \left(\boldsymbol{J}^{\mathrm{H}}\boldsymbol{\Pi}_{\bar{\boldsymbol{A}}}^{\perp}\boldsymbol{J}\right)\right\}. \tag{23}$$

Substituting (18), (20) – (23) into (15), the CRB in the PR model for the desired direction θ, which corresponds to the entry $C_{\theta\theta}$, is calculated using the block matrix inversion lemma as follows (see [15, Misc. 7.3],[16, Eq. (R.3)-(R.4)])

$$\begin{aligned}
&\text{PR-CRB} = C_{\theta\theta} \\
&= \frac{\nu}{2T}\Big(\mathrm{Re}\left\{\bar{M}_{11}\boldsymbol{d}^{\mathrm{H}}\boldsymbol{\Pi}_{\bar{\boldsymbol{A}}}^{\perp}\boldsymbol{d}\right\} - \mathrm{Re}\Big\{\left(\bar{\boldsymbol{M}}_{21}^{\mathrm{H}} \otimes \left(\boldsymbol{d}^{\mathrm{H}}\boldsymbol{\Pi}_{\bar{\boldsymbol{A}}}^{\perp}\boldsymbol{J}\right)\right) \\
&\left(\bar{\boldsymbol{M}}_{22}^{-1} \otimes \left(\boldsymbol{J}^{\mathrm{H}}\boldsymbol{\Pi}_{\bar{\boldsymbol{A}}}^{\perp}\boldsymbol{J}\right)^{-1}\right)\left(\bar{\boldsymbol{M}}_{21} \otimes \left(\boldsymbol{J}^{\mathrm{H}}\boldsymbol{\Pi}_{\bar{\boldsymbol{A}}}^{\perp}\boldsymbol{d}\right)\right)\Big\}\Big)^{-1} \\
&= \frac{\nu}{2T}\left(\bar{M}_{11}\boldsymbol{d}^{\mathrm{H}}\boldsymbol{\Pi}_{\bar{\boldsymbol{A}}}^{\perp}\boldsymbol{d} - \left(\bar{\boldsymbol{M}}_{21}^{\mathrm{H}}\bar{\boldsymbol{M}}_{22}^{-1}\bar{\boldsymbol{M}}_{21}\right)\boldsymbol{d}^{\mathrm{H}}\boldsymbol{\Pi}_{\boldsymbol{\Pi}_{\bar{\boldsymbol{A}}}^{\perp}\boldsymbol{J}}\boldsymbol{d}\right)^{-1}.
\end{aligned} \tag{24}$$

Furthermore, we can prove that $\boldsymbol{\Pi}_{\bar{\boldsymbol{A}}}^{\perp} = \boldsymbol{\Pi}_{\boldsymbol{\Pi}_{\bar{\boldsymbol{A}}}^{\perp}\boldsymbol{J}}$ by noting, due to the existence of the CRB matrix $\boldsymbol{C}$, $\boldsymbol{J}^{\mathrm{H}}\boldsymbol{\Pi}_{\bar{\boldsymbol{A}}}^{\perp}\boldsymbol{J}$ is invertible and hence rank$(\boldsymbol{\Pi}_{\bar{\boldsymbol{A}}}^{\perp})$ = rank$(\boldsymbol{\Pi}_{\boldsymbol{\Pi}_{\bar{\boldsymbol{A}}}^{\perp}\boldsymbol{J}}) = M - N$. Moreover, the two idempotent Hermitian matrices $\boldsymbol{\Pi}_{\bar{\boldsymbol{A}}}^{\perp}$ and $\boldsymbol{\Pi}_{\boldsymbol{\Pi}_{\bar{\boldsymbol{A}}}^{\perp}\boldsymbol{J}}$ are commutative and hence they share the same eigenvectors [15, Th. 1.3.12]. Every vector lying in the nullspace of $\boldsymbol{\Pi}_{\bar{\boldsymbol{A}}}^{\perp}$ also lies in the nullspace of $\boldsymbol{\Pi}_{\boldsymbol{\Pi}_{\bar{\boldsymbol{A}}}^{\perp}\boldsymbol{J}}$ and therefore the two projection matrices must be identical. As a result, the CRB for the desired parameter θ simplifies to:

$$\text{PR-CRB} = \frac{\nu}{2T}\left(\left(\bar{M}_{11} - \bar{\boldsymbol{M}}_{21}^{\mathrm{H}}\bar{\boldsymbol{M}}_{22}^{-1}\bar{\boldsymbol{M}}_{21}\right)\boldsymbol{d}^{\mathrm{H}}\boldsymbol{\Pi}_{\bar{\boldsymbol{A}}}^{\perp}\boldsymbol{d}\right)^{-1}. \tag{25}$$

The expression in (25) is further rewritten by noting that the transformation matrix $\boldsymbol{T}$ in (6) is invertible, and therefore $\boldsymbol{\Pi}_{\bar{\boldsymbol{A}}}^{\perp} = \boldsymbol{\Pi}_{\boldsymbol{A}}^{\perp}$. In addition, substituting $\bar{\boldsymbol{M}} = \left(\boldsymbol{T}^{-1}\right)^{*}\boldsymbol{M}\boldsymbol{T}^{-\mathrm{T}}$ to (25) and simplifying, we obtain the following expression for the CRB for the DOA of the desired source signal in the PR case:

$$\text{PR-CRB} = \frac{\nu}{2T}\left(\left(M_{11} - \boldsymbol{M}_{21}^{\mathrm{H}}\boldsymbol{M}_{22}^{-1}\boldsymbol{M}_{21}\right)\boldsymbol{d}^{\mathrm{H}}\boldsymbol{\Pi}_{\boldsymbol{A}}^{\perp}\boldsymbol{d}\right)^{-1}. \tag{26}$$

where the matrix $\boldsymbol{M}$ is defined and partitioned conformably with the matrix $\bar{\boldsymbol{M}}$ in (17) as

$$\boldsymbol{M} = \left(\boldsymbol{P}\boldsymbol{A}^{\mathrm{H}}\boldsymbol{R}^{-1}\boldsymbol{A}\boldsymbol{P}\right)^{\mathrm{T}} = \begin{bmatrix} M_{11} & \boldsymbol{M}_{21}^{\mathrm{H}} \\ \boldsymbol{M}_{21} & \boldsymbol{M}_{22}\end{bmatrix}. \tag{27}$$

5. ASYMPTOTIC RESULTS

In this section, four propositions that relate the DOA estimation error performance of estimators using the PR model with that of the conventional model are presented.

Proposition 1. *The Cramér-Rao Bound of the PR model is always lower-bounded by the Cramér-Rao Bound of the conventional model*

Sketch of Proof. If we choose $\theta = \theta_1$, it is sufficient to prove that PR-CRB $\geq$ CRB$_{11}$, where the inverse of the CRB matrix of the conventional model is given by [7]:

$$\text{CRB}^{-1} = \frac{2T}{\nu}\mathrm{Re}\left\{\begin{bmatrix} M_{11} & \boldsymbol{M}_{21}^{\mathrm{H}} \\ \boldsymbol{M}_{21} & \boldsymbol{M}_{22}\end{bmatrix} \odot \left(\boldsymbol{D}^{\mathrm{H}}\boldsymbol{\Pi}_{\boldsymbol{A}}^{\perp}\boldsymbol{D}\right)\right\}, \tag{28}$$

where $\boldsymbol{D} = \left[\frac{d\boldsymbol{a}(\theta_1)}{d\theta_1}, \ldots, \frac{d\boldsymbol{a}(\theta_N)}{d\theta_N}\right] = [\boldsymbol{d}\,|\,\boldsymbol{D}_2]$ and $\odot$ denotes the Hadamard product. Correspondingly, we partition

$$\boldsymbol{D}^{\mathrm{H}}\boldsymbol{\Pi}_{\boldsymbol{A}}^{\perp}\boldsymbol{D} = \begin{bmatrix} \boldsymbol{d}^{\mathrm{H}}\boldsymbol{\Pi}_{\boldsymbol{A}}^{\perp}\boldsymbol{d} & \boldsymbol{d}^{\mathrm{H}}\boldsymbol{\Pi}_{\boldsymbol{A}}^{\perp}\boldsymbol{D}_2 \\ \boldsymbol{D}_2^{\mathrm{H}}\boldsymbol{\Pi}_{\boldsymbol{A}}^{\perp}\boldsymbol{d} & \boldsymbol{D}_2^{\mathrm{H}}\boldsymbol{\Pi}_{\boldsymbol{A}}^{\perp}\boldsymbol{D}_2\end{bmatrix} = \begin{bmatrix} \bar{D}_{11} & \bar{\boldsymbol{D}}_{21}^{\mathrm{H}} \\ \bar{\boldsymbol{D}}_{21} & \bar{\boldsymbol{D}}_{22}\end{bmatrix}, \tag{29}$$

and define $\tilde{\boldsymbol{M}} = \begin{bmatrix} \boldsymbol{M}_{21}^{\mathrm{H}}\boldsymbol{M}_{22}^{-1/2} \\ \boldsymbol{M}_{22}^{1/2}\end{bmatrix}\begin{bmatrix}\boldsymbol{M}_{22}^{-1/2}\boldsymbol{M}_{21} & \boldsymbol{M}_{22}^{1/2}\end{bmatrix}$. From [17, Lemma A.1], the following expression

$$\begin{aligned}
&\mathrm{Re}\left\{\tilde{\boldsymbol{M}} \odot \left(\boldsymbol{D}^{\mathrm{H}}\boldsymbol{\Pi}_{\boldsymbol{A}}^{\perp}\boldsymbol{D}\right)\right\} = \\
&\mathrm{Re}\left\{\begin{bmatrix} \left(\boldsymbol{M}_{21}^{\mathrm{H}}\boldsymbol{M}_{22}^{-1}\boldsymbol{M}_{12}\right)\bar{D}_{11} & \boldsymbol{M}_{21}^{\mathrm{H}} \odot \bar{\boldsymbol{D}}_{21}^{\mathrm{H}} \\ \boldsymbol{M}_{21} \odot \bar{\boldsymbol{D}}_{21} & \boldsymbol{M}_{22} \odot \bar{\boldsymbol{D}}_{22}\end{bmatrix}\right\}
\end{aligned} \tag{30}$$

is positive semidefinite. Applying the property of the Schur complement of the most upper-left entry of the block matrix on the right hand side of (30) results in (see [18, (6.5)]):

$$\begin{aligned}
&\mathrm{Re}\left\{\left(M_{11} - \boldsymbol{M}_{21}^{\mathrm{H}}\boldsymbol{M}_{22}^{-1}\boldsymbol{M}_{21}\right)\bar{D}_{11}\right\} \leq \mathrm{Re}\left\{M_{11}\bar{D}_{11}\right\} - \\
&\mathrm{Re}\left\{\boldsymbol{M}_{21}^{\mathrm{H}} \odot \bar{\boldsymbol{D}}_{21}^{\mathrm{H}}\right\}\mathrm{Re}\left\{\boldsymbol{M}_{22} \odot \bar{\boldsymbol{D}}_{22}\right\}^{-1}\mathrm{Re}\left\{\boldsymbol{M}_{21} \odot \bar{\boldsymbol{D}}_{21}\right\}.
\end{aligned} \tag{31}$$

Note that both expressions on the left and the right hand side of (31) are nonnegative. Consequently, taking the inverse of both sides and applying the block matrix inversion lemma for the most upper-left entry of the matrix on the right hand side results in

$$\begin{aligned}
&\mathrm{Re}\left\{\left(M_{11} - \boldsymbol{M}_{21}^{\mathrm{H}}\boldsymbol{M}_{22}^{-1}\boldsymbol{M}_{21}\right)\bar{D}_{11}\right\}^{-1} \geq \\
&\left[\mathrm{Re}\left\{\begin{bmatrix} M_{11} & \boldsymbol{M}_{21}^{\mathrm{H}} \\ \boldsymbol{M}_{21} & \boldsymbol{M}_{22}\end{bmatrix} \odot \begin{bmatrix} \bar{D}_{11} & \bar{\boldsymbol{D}}_{21}^{\mathrm{H}} \\ \bar{\boldsymbol{D}}_{21} & \bar{\boldsymbol{D}}_{22}\end{bmatrix}\right\}^{-1}\right]_{11},
\end{aligned} \tag{32}$$

From (26), (28), (29) and (32), the result follows. $\square$

Proposition 2. *In the case of high SNR and uncorrelated source signals, the Cramér-Rao Bound for the PR model is approximately equal to the conventional Cramér-Rao Bound*

Sketch of Proof. In the high SNR regime and uncorrelated source signals, the matrix $\boldsymbol{M}$ defined in (27) is element-wise approximately equal to the diagonal matrix $\boldsymbol{P}$ (see [19, Eq. (8.110)]), and thus the conventional CRB is reduced to CRB$_{11} \approx \frac{\nu}{2T}\left(\boldsymbol{d}^{\mathrm{H}}\boldsymbol{\Pi}_{\boldsymbol{A}}^{\perp}\boldsymbol{d}P_{11}\right)^{-1}$. On the other hand, since the source signals are uncorrelated, $\boldsymbol{M}_{21} \approx \boldsymbol{P}_{21} = \boldsymbol{0}$. As a result, the CRB for the PR model in (26) is given by PR-CRB $= \frac{\nu}{2T}\left(P_{11}\boldsymbol{d}^{\mathrm{H}}\boldsymbol{\Pi}_{\boldsymbol{A}}^{\perp}\boldsymbol{d}\right)^{-1}$ and the result follows. $\square$

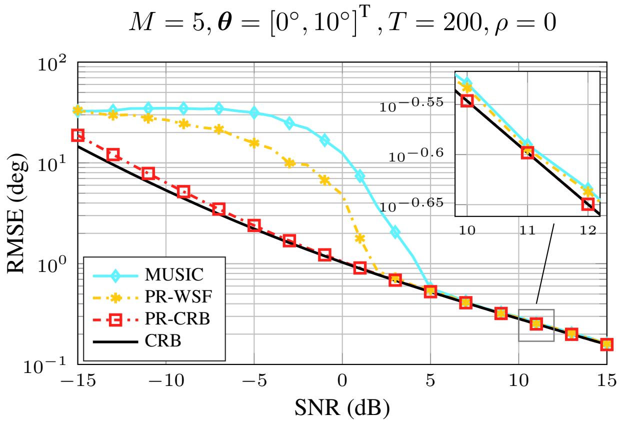

Fig. 1: Uncorrelated signals, number of snapshots $T = 200$

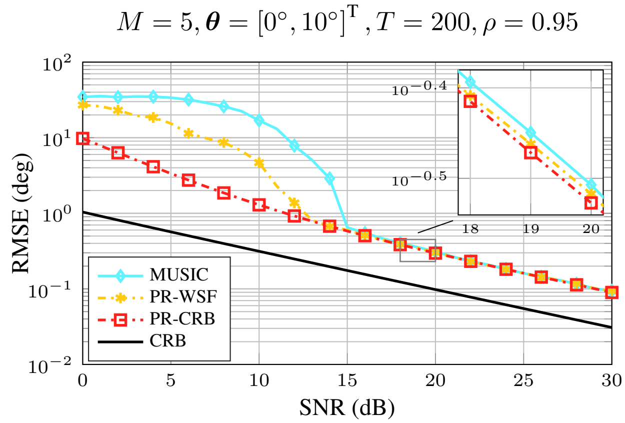

Fig. 2: Correlated signals, number of snapshots $T = 200$

Proposition 3. *As $T \to \infty$, the mean-square error of the partially-relaxed weighted subspace fitting (PR-WSF) estimator in [3] achieves the Cramér-Rao Bound of the PR model.*

Sketch of Proof. By choosing a special weighting matrix as described in [3, Eq. (14)] for the PR-WSF estimator, the pq-th element of the asymptotic inverse error covariance matrix $\boldsymbol{C}^{-1}$ with respect to the parameter $\boldsymbol{\beta}$ defined in Section 4 is given by (see [20, Eq. (50)–(51) and (70)]):

$$\left[\boldsymbol{C}^{-1}\right]_{pq} = \frac{2T}{\nu}\mathrm{Re}\left\{\mathrm{tr}\left(\frac{d\bar{\boldsymbol{A}}}{d\beta_p}^{\mathrm{H}}\boldsymbol{\Pi}_{\bar{\boldsymbol{A}}}^{\perp}\frac{d\bar{\boldsymbol{A}}}{d\beta_q}\bar{\boldsymbol{A}}^{\dagger}\boldsymbol{E}_{\mathrm{s}}\boldsymbol{W}_{\mathrm{opt}}\boldsymbol{E}_{\mathrm{s}}^{\mathrm{H}}\bar{\boldsymbol{A}}^{\dagger\mathrm{H}}\right)\right\}, \tag{33}$$

with $\boldsymbol{E}_{\mathrm{s}}$ and $\boldsymbol{W}_{\mathrm{opt}}$ defined in [20, Eq. (10)] and [20, Eq. (71)], respectively. Furthermore, we have $\bar{\boldsymbol{A}}^{\dagger}\boldsymbol{E}_{\mathrm{s}}\boldsymbol{W}_{\mathrm{opt}}\boldsymbol{E}_{\mathrm{s}}^{\mathrm{H}}\bar{\boldsymbol{A}}^{\dagger\mathrm{H}} = \bar{\boldsymbol{P}}\bar{\boldsymbol{A}}^{\mathrm{H}}\boldsymbol{R}^{-1}\bar{\boldsymbol{A}}\bar{\boldsymbol{P}}$ by a similar argument as in [20, Th. 3]. Comparing (33) with (14), the result follows. □

Proposition 4. *As $T \to \infty$, the mean-square error of PR-WSF is smaller than or equal to that of MUSIC.*

Sketch of Proof. If we choose the weighting matrix $\boldsymbol{W} = \boldsymbol{I}_N$, the estimator PR-WSF is equivalent to MUSIC [3, App. B]. However, by a similar argument as in [20, Th. 3], the weighting matrix of PR-WSF results in the smallest asymptotic mean square error. Consequently, as $T \to \infty$, the mean square error of PR-WSF is always smaller than or equal to that of MUSIC. □

6. SIMULATION RESULTS

In this section, we provide some simulation results for the stochastic CRB and the proposed CRB for the relaxed array manifold case (PR-CRB) in (26). The results are averaged over $N_R = 1000$ Monte-Carlo runs. The Root-Mean-Squared-Error (RMSE) is calculated as:

$$\mathrm{RMSE} = \sqrt{\frac{1}{N_R N}\sum_{\omega=1}^{N_R}\sum_{n=1}^{N}\left(\hat{\theta}_n^{(\omega)} - \theta_n\right)^2}, \tag{34}$$

where the estimated DOAs in the ω-th Monte-Carlo run $\hat{\boldsymbol{\theta}}^{(\omega)} = [\hat{\theta}_1^{(\omega)}, \ldots, \hat{\theta}_N^{(\omega)}]^{\mathrm{T}}$ and the true DOAs $\boldsymbol{\theta} = [\theta_1, \ldots, \theta_N]^{\mathrm{T}}$ in (34) are sorted in ascending order. We assume $N = 2$ source signals at $\boldsymbol{\theta} = [0°, 10°]^{\mathrm{T}}$ with the transmit covariance matrix $\boldsymbol{P} = \begin{bmatrix}1 & \rho^* \\ \rho & 1\end{bmatrix}$ impinge on a ULA of $M = 5$ antennas with the spacing equal to half of the signal wavelength. The number of snapshots is kept at $T = 200$. Since the asymptotic performance of root-MUSIC[21] and MUSIC are identical [23], and the mean-square error of MUSIC estimates is smaller than or equal to that of ESPRIT [24], we only depict the error performance of MUSIC. In the first scenario depicted in Figure 1, when the two source signals are uncorrelated, the difference between the two Cramér-Rao Bounds are significant if the SNR is very low, as predicted by Proposition 2. PR-WSF outperforms MUSIC in both the threshold and the asymptotic regions. The fact that the MUSIC estimator is outperformed by PR-WSF in the asymptotic region is predicted by Proposition 4, although the difference in the RMSE performance is negligible.

In Figure 2, we assume that the two source signals are correlated with the correlation factor $\rho = 0.95$. As predicted by Proposition 1, we observe that the Cramér-Rao Bound for the conventional signal model is smaller than that of the partial relaxation model. Moreover, the difference in RMSE between the two Cramér-Rao Bounds is imminent in the whole inspected region. Similar to the first scenario, PR-WSF outperforms MUSIC in both the asymptotic and the threshold regions.

7. CONCLUSIONS AND OUTLOOK

In this paper, a non-redundant parameterization for the signal model under the relaxed steering matrix assumption is introduced, and henceforth, the Cramér-Rao Bound for the PR model is derived. Theoretical and numerical results show that, if the source signals are uncorrelated, the Cramér-Rao Bound of the PR model, which is achieved asymptotically by the computationally-efficient PR-WSF, is comparable to that of the conventional counterpart. Furthermore, asymptotically, PR-WSF possesses a lower mean-square error than MUSIC.

For future work, the theoretical error behaviors for the remaining estimators under the PR framework, not only in the asymptotic region but also in the threshold region, are of great interest and thus require further investigations.

8. REFERENCES

[1] M. Trinh-Hoang, M. Viberg, and M. Pesavento, "Improved DOA Estimators Using Partial Relaxation Approach," in *2017 IEEE 7th International Workshop on Computational Advances in Multi-Sensor Adaptive Processing (CAMSAP)*, Dec 2017, pp. 1–5.

[2] M. Trinh-Hoang, M. Viberg, and M. Pesavento, "An Improved DOA Estimator Based on Partial Relaxation Approach," in *2018 IEEE International Conference on Acoustics, Speech and Signal Processing (ICASSP)*, Apr 2018, pp. 3246–3250.

[3] M. Trinh-Hoang, M. Viberg, and M. Pesavento, "Partial Relaxation Approach: An Eigenvalue-Based DOA Estimator Framework," *IEEE Transactions on Signal Processing*, 2018.

[4] A. Paulraj, B. Ottersten, R. Roy, A. Swindlehurst, G. Xu, and T. Kailath, "Subspace Methods for Directions-Of-Arrival Estimation," *Handbook of Statistics*, vol. 10, pp. 693 – 739, 1993.

[5] Pei-Jung Chung, Mats Viberg, and Jia Yu, "Chapter 14 - DOA Estimation Methods and Algorithms," in *Volume 3: Array and Statistical Signal Processing*, Rama Chellappa Abdelhak M. Zoubir, Mats Viberg and Sergios Theodoridis, Eds., vol. 3 of *Academic Press Library in Signal Processing*, pp. 599 – 650. Elsevier, 2014.

[6] R.O. Schmidt, "Multiple Emitter Location and Signal Parameter Estimation," *IEEE Transactions on Antennas and Propagation*, vol. 34, no. 3, pp. 276–280, Mar 1986.

[7] P. Stoica and A. Nehorai, "Performance Study of Conditional and Unconditional Direction-of-Arrival Estimation," *IEEE Transactions on Acoustics, Speech, and Signal Processing*, vol. 38, no. 10, pp. 1783–1795, Oct 1990.

[8] P. Stoica, E. G. Larsson, and A. B. Gershman, "The Stochastic CRB for Array Processing: A Textbook Derivation," *IEEE Signal Processing Letters*, vol. 8, no. 5, pp. 148–150, May 2001.

[9] Jean Pierre Delmas, "Chapter 16 - Performance Bounds and Statistical Analysis of DOA Estimation," in *Academic Press Library in Signal Processing: Volume 3*, Abdelhak M. Zoubir, Mats Viberg, Rama Chellappa, and Sergios Theodoridis, Eds., vol. 3 of *Academic Press Library in Signal Processing*, pp. 719 – 764. Elsevier, 2014.

[10] H. Cramér, *Mathematical Methods of Statistics*, Princeton University Press, 1945.

[11] C. R. Rao, "Information and Accuracy Attainable in the Estimation of Statistical Parameters," *Bulletin of Calcutta Mathematical Society*, vol. 37, pp. 81–91, 1945.

[12] Brian M. Sadler and Terrence J. Moore, "Chapter 8 - Performance Analysis and Bounds," in *Academic Press Library in Signal Processing: Volume 3*, Abdelhak M. Zoubir, Mats Viberg, Rama Chellappa, and Sergios Theodoridis, Eds., vol. 3 of *Academic Press Library in Signal Processing*, pp. 297 – 322. Elsevier, 2014.

[13] Thomas J. Rothenberg, "Identification in Parametric Models," *Econometrica*, vol. 39, no. 3, pp. 577–591, 1971.

[14] A. B. Gershman, P. Stoica, M. Pesavento, and E. G. Larsson, "Stochastic Cramer-Rao Bound for Direction Estimation in Unknown Noise Fields," *IEE Proceedings - Radar, Sonar and Navigation*, vol. 149, no. 1, pp. 2–8, Feb 2002.

[15] Roger A. Horn and Charles R. Johnson, *Matrix Analysis*, Cambridge University Press, New York, NY, USA, 2nd edition, 2012.

[16] P. Stoica and A. Nehorai, "MUSIC, Maximum Likelihood, and Cramer-Rao bound," *IEEE Transactions on Acoustics, Speech, and Signal Processing*, vol. 37, no. 5, pp. 720–741, May 1989.

[17] P. Stoica and A. Nehorai, "MUSIC, Maximum Likelihood, and Cramer-Rao Bound: Further Results and Comparisons," *IEEE Transactions on Acoustics, Speech, and Signal Processing*, vol. 38, no. 12, pp. 2140–2150, Dec 1990.

[18] Charles R. Johnson, *Matrix Theory and Applications*, AMS Short Course Lecture Notes. American Mathematical Society, 1990.

[19] H. L. Van Trees, *Optimum Array Processing*, Wiley, New York, 2002.

[20] M. Viberg and B. Ottersten, "Sensor Array Processing Based on Subspace Fitting," *IEEE Transactions on Signal Processing*, vol. 39, no. 5, pp. 1110–1121, May 1991.

[21] A Barabell, "Improving the Resolution Performance of Eigenstructure-based Direction-Finding Algorithms," in *IEEE International Conference on Acoustics, Speech, and Signal Processing*, Apr 1983, vol. 8, pp. 336–339.

[22] R. Roy and T. Kailath, "ESPRIT-Estimation of Signal Parameters via Rotational Invariance Techniques," *IEEE Transactions on Acoustics, Speech and Signal Processing*, vol. 37, no. 7, pp. 984–995, Jul 1989.

[23] B. D. Rao and K. V. S. Hari, "Performance Analysis of Root-Music," *IEEE Transactions on Acoustics, Speech, and Signal Processing*, vol. 37, no. 12, pp. 1939–1949, Dec 1989.

[24] P. Stoica and A. Nehorai, "Performance Comparison of Subspace Rotation and MUSIC Methods for Direction Estimation," *IEEE Transactions on Signal Processing*, vol. 39, no. 2, pp. 446–453, Feb 1991.